

Sensorless Control with Friction and Human Intention Estimation of Exoskeleton Robot for Upper-limb Rehabilitation

Lee-Kai Liu, Tzu-Chieh Chien, Yi-Lian Chen, Li-Chen Fu, *Fellow, IEEE*, and Jin-Shin Lai

Abstract—In this paper, for the control problem of upper-limb rehabilitation using exoskeleton robot, we propose a sensorless control scheme with human intention estimation. In order to implement the active mode rehabilitation therapy, an interactive torque observer using Kalman filter is utilized to obtain human intention on the human-robot interaction control. Since the accurate friction model is crucial for constructing the observer, a deep neural network (DNN) is proposed in this study to obtain an accurate friction model. Furthermore, a variable admittance model is constructed to derive human intention to the desired motion trajectory. Various experiments have been conducted to verify the performance of the proposed control scheme based on the interactive torque observer.

I. INTRODUCTION

Some studies show that many neurological or orthopedic disorders, such as stroke, may cause the motor impairments on the upper-limb [1], [2]. This may result in muscle weakness, limited range of motion (ROM), or lack of muscle control. Compared with traditionally manual rehabilitation therapy, the robot-assisted therapy has the potential to provide intensive rehabilitation consistently for a longer duration [3] and regardless of the skills and fatigue level of the therapists. Furthermore, the robot-assisted device can accurately measure quantitative, bio-medical and kinetic information by the sensor to evaluate the patients condition. These issues of developing robot-assisted therapy motivate more and more researchers dedicated to it [4]. In general, there are two kinds of robots used in upper-limb rehabilitation, which are the end-effector robot and the exoskeleton. Regarding that end-effector robot is hard to determine the posture of the upper-limb and to analyze the interaction force in each joint, robotic therapy research has shifted towards exoskeleton robots recently. The advantages of the exoskeleton robot are offering a large range of motion and applying torque to each individual joint. Besides, the pre-defined robot posture can help to regulate the joint configuration of humans upper-limb so that the effect of synergy pattern will be minimized.

The therapeutic exercise of robot-assisted rehabilitation basically can be divided into 4 types, namely, passive, active-assistive, active and active-resistive [5], which are similar to those conventional rehabilitation programs. Since the active mode requires the robot to be able to follow the human

L.-K. Liu, Tzu-Chieh Chien, Yi-Lian Chen, are with the Department of Electrical Engineering, National Taiwan University (NTU), Taiwan, R.O.C.

L.-C. Fu is with the Department of Electrical Engineering and Department of Computer Science and Information Engineering, National Taiwan University, Taiwan, R.O.C (e-mail: lichen@ntu.edu.tw)

J.-S. Lai is with the Department of Physical Medicine and Rehabilitation, NTU and NTU Hospital, R.O.C. (e-mail: jslai@ntu.edu.tw)

movements and conduct a suitable human-robot interaction, the human intention extraction becomes an important issue for robot control. In general, there are two main sensors used to acquire the human intention which are the force/torque sensor (F/T sensor) and the surface electromyography (sEMG) sensor. By using the F/T sensor, EXO-UL7 [6] applied admittance model between interaction force and position difference to get the desired position input. The main disadvantage of using F/T sensor is that most F/T sensors are placed only on the links corresponding to the human upper arm, forearm or hand due to the mechanical structure difficulty. This implies that the human-robot interactive force will be undetected when the contacts do not occur at the sensors locations. In [7], the frequency analysis of the sEMG signal is used to estimate the patient's intention. However, the poor signal-to-noise ratio of sEMG sensors makes the online extraction of intentional features more difficult. Moreover, it often takes a long time to connect sEMG sensor with the user due to the requirement of precise placement.

Regarding the disadvantages of both sensors, the interactive torque observer combined with sEMG has been proposed in our previous work [8] and utilized in the active mode control. However, the friction model in [8] is a traditional Coulomb friction model which cannot precisely describe the friction model of the exoskeleton and sometimes leads to the unsatisfactory performance of interactive torque observer. Additionally, the active mode control in [8] is an open loop control which may result in the non-smooth movement.

In order to solve the problems mentioned above, we propose a sensorless exoskeleton robot control scheme integrated with interactive torque observer and Deep Neural Network (DNN) friction model estimation in this paper. Here, sensorless means that we do not use additional sensors to acquire human intention, but the motor encoder and current information are still employed. The proposed control scheme is implemented on the NTUH-II, which is a self-built upper-limb rehabilitation robot, to conduct the active mode therapy. Inspired by [10], the interactive torque observer constructed in this paper utilizes the Kalman filter to deal with the system uncertainties and measurement noise. Moreover, we propose a DNN based friction model to obtain a more accurate friction estimation. In the exoskeleton robot field, the friction model is sometimes not as simple as the traditional model but contains nonlinear and complicated environmental factors. The DNN based friction model proposed in this paper is a novel way to obtain a more precise friction estimation in this situation. We integrate the interactive torque observer, the variance admittance model, and the feedforward PID

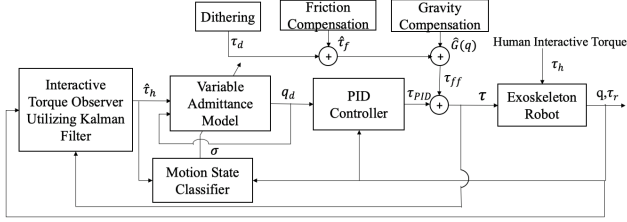


Fig. 1. Control system block for active mode therapy

controller to construct the proper control scheme in order to conduct the active mode therapy. The performance of the interactive torque observer and the whole control scheme are evaluated in the experiment result which shows the capability of the observer to replace the additional sensors and the capability of the control scheme to conduct a fine therapy movement.

The rest of this paper is organized in the following order. In Section II, the problem formulation and the system overview is provided. The methodology of this study is proposed in Section III. To evaluate the control scheme performance, the experimental protocols and results are presented in Section IV. Finally, the conclusion is in Section V.

II. PRELIMINARY & SYSTEM OVERVIEW

In this paper, we consider the active mode rehabilitation therapy, which is, the robot needs to follow the human intention to complete the therapy movement. We can separate the whole problem into two sub-problems. The first sub-problem is how to extract the motion intention of the patient. Instead of using additional sensor, we construct an interactive torque observer utilizing Kalman filter to obtain the motion intention in Section III. Moreover, an accurate friction model of the exoskeleton is needed to build the observer. Thus, we construct a DNN based friction model to obtain the friction estimation. The second sub-problem is how to translate the human intention into the desired trajectory. We construct a variable admittance model in order to strike a balance between the force required to move the robot and the ability to perform fine movements.

A. System Overview

To deal with the problems in the previous paragraph, we construct a control structure which is shown in Fig. 1. The details of this structure will be discussed as follows. First, we can obtain the joint angle q , angular velocity \dot{q} and the motor torque τ_r from the motor sensor equipped on the exoskeleton. Next, the estimated interactive torque $\hat{\tau}_h$ comes from the interactive torque observer which will be introduced in Section III-B. Then, the desired trajectory q_d is generated by the variance admittance model with the estimated interactive torque $\hat{\tau}_h$, motion state σ and the previous trajectory information \ddot{q}_d . The details of the variable admittance model will be shown in Section III-C. The desired trajectory is sent into the PID controller, and the output of the PID controller τ is a combination of feed-forward and feedback signal. The feed-forward signal includes the friction

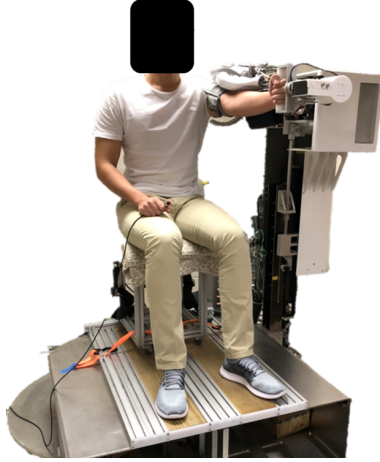


Fig. 2. NTUH-II exoskeleton robot.

estimation $\hat{\tau}_f$, joint gravity estimation $\hat{G}(q)$ and dithering signal τ_d . The first two components aim to make the robot response faster, and the third one aim to reduce the initial force the subject need to push the robot from static. The discussion of friction estimation and dithering signal will be introduced in Section III-A and Section III-D, respectively. In summary, the overall control scheme has the advantage that the robot has high responsiveness and the movement is smooth.

B. Exoskeleton Robot: NTUH-II

The whole control scheme is built on NTUH-II(Fig. 2) which is a self-built exoskeleton [9]. NTUH-II has 8 degrees of freedom (DOF) and is applicable for either side of upper-limb rehabilitation. The control strategy in this paper is based on the interactive torque observer for human intention detection, however, the interactive torque observer cannot be applied to shoulder external/internal rotation (ER) joint under the current mechanical design of NTUH-II. Therefore, we focus on realizing our method on shoulder horizontal abduction/adduction (HABD), shoulder flexion/extension (SF) and elbow flexion/extension (EF) joint.

III. METHODOLOGY

In this section, the interactive torque observer utilized Kalman filter is constructed. First, the detail of the robot friction model estimation will be introduced. After having the completed dynamics model of the robot, we construct an interactive torque observer in Section III-B. Further, the proposed variable admittance model will be shown in Section III-C. Regarding the limitation of interactive torque observer when the robot joints are static, we add the dithering signal which will be explained in Section III-D.

A. Friction Modeling and Estimation

Since the formulation of manipulator dynamics derived by the Newton-Euler method is lack of the friction term, building the friction model separately is needed to complete the robot dynamics model. The estimated friction model plays a two-fold role in our system. First, since the exoskeleton robot usually runs with low acceleration and velocity, the

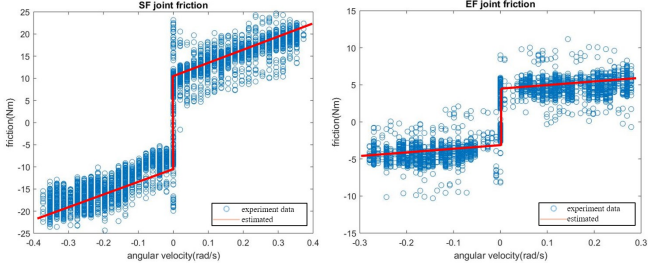


Fig. 3. The experiment result of SF and EF joint.

friction effects are dominating. Due to above, an accurate friction model in the dynamics model is crucial to estimate the interactive torque. The second one is that feed-forwarding a portion of the friction torque can make the robot have high responsiveness.

In order to find out friction characteristic, an experiment is performed on each joint. The joints move forward and backward at some constant velocities. From Fig. 3, the characteristics of Coulomb friction and viscous friction of SF joint and EF joint are clearly visible. Therefore, the friction model of these joints except for HABD joint can be expressed as

$$\hat{\tau}_{f,i} = \text{sgn}(\dot{q}_i) \cdot \tau_{c,i} + \tau_{v,i} \cdot \dot{q}_i \quad (1)$$

where $\hat{\tau}_{f,i}$ is the estimated friction. $\tau_{c,i}$ and $\tau_{v,i}$ mean the Coulomb friction and viscous friction coefficients in the i -th joint, respectively.

Due to the unique mechanical design of NTUH-II, the friction of HABD joint includes the contact friction of rollers attached to the chassis. This makes the friction model of HABD joint not only include the friction from the motor but also from the environment. Hence, we propose a machine learning method which is called DNN to model the friction of HABD joint. Fig. 4 shows the mechanical design of HABD joint as well as the details of the rollers and also shows the definition of the rollers coordinate. HABD joint moves in the XY-plane and the rollers rotate along the Z-axis during the movement. The left part of Fig. 5 is the experiment result of HABD joint friction which is conducted while the movement is with constant velocity. The x -axis is the angle and the y -axis is the friction. First, the rollers rotating process can be separated into two phases. In phase 1, the friction continuously increases until the movement direction and rollers pose are orthogonal. In phase 2, it further decreases until the rollers rotating process is completed. Apparently, the traditional friction model cannot express this kind of characteristic. According to the potential ability of the DNN model, it can automatically find the highly nonlinear relationship between the input and the output data. By using the grid search, the best structures of the DNN model can be constructed with 3 hidden layers, and each layer contains 20 neurons. The output of the network is the estimation friction $\hat{\tau}_{f,i}$. The input vector of the DNN model is the velocity and the relative angle which indicates moving angle after the last velocity reversing of HABD joint. These two inputs are reasonably chosen because the velocity relates to the viscous friction and the relative angle relates to the timing

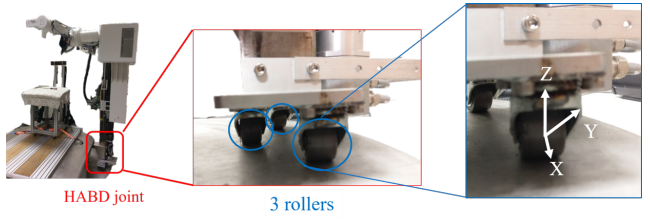


Fig. 4. Mechanical design of HABD joint and the rollers.

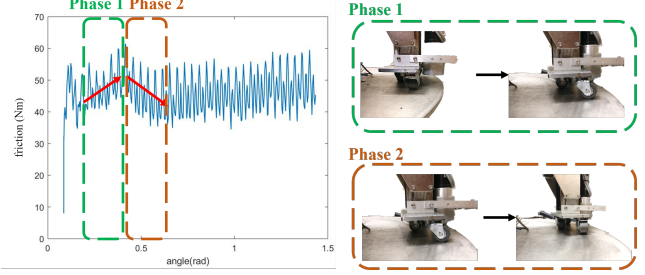


Fig. 5. The relationship between experiment result of HABD joint friction and the rollers rotating process.

of the rollers are rotating or not. Note that the activation function is hyperbolic tangent. The number of total data for the experiment is 28000, and 85% data are split for training, and 15% data split for validation. The highest root-mean-square error of validation can be lower than 5.6 (Nm).

Combine the friction estimation $\hat{\tau}_f$ into an n DOFs manipulator, the dynamics equation can be expressed as

$$M(\mathbf{q})\ddot{\mathbf{q}} + C(\mathbf{q}, \dot{\mathbf{q}})\dot{\mathbf{q}} + \mathbf{G}(\mathbf{q}) + \hat{\tau}_f = \tau_m \quad (2)$$

where $\mathbf{q}, \dot{\mathbf{q}}, \ddot{\mathbf{q}} \in \mathbb{R}^n$ denote vectors of joint angle, angular velocity, and angular acceleration of the exoskeleton robot arm, respectively. Furthermore, $M(\mathbf{q})$, $C(\mathbf{q}, \dot{\mathbf{q}})\dot{\mathbf{q}}$, and $\mathbf{G}(\mathbf{q})$ represent the inertia matrix, Centrifugal/Coriolis, and gravity matrices of exoskeleton robot arm. τ_m is the motor torque vector.

B. Interactive Torque Observer Utilizing Kalman Filter

In order to detect the interactive torque between the human and robot without the additional sensor (e.g. F/T sensor), we apply an interactive torque observer utilizing Kalman filter [10] on NTUH-II. In [10], the observer is only verified by simulation results of a dual-arm collaborative robot. In this paper, we utilize the interactive torque observer on an exoskeleton to conduct the active mode therapy. The benefit of the observer can be summarized into two points. First, uncertainties of the manipulators dynamics model and measurement noise will be taken into account. Second, this observer has more degrees of freedom compared with traditional observer [11]. In this section, we will show how to construct it step by step.

The robot dynamics is described by

$$M(\mathbf{q})\ddot{\mathbf{q}} + C(\mathbf{q}, \dot{\mathbf{q}})\dot{\mathbf{q}} + \mathbf{G}(\mathbf{q}) + \tau_f = \tau_m + \tau_h \quad (3)$$

which is similar to (2) except for the term τ_h which is the interactive torque between human and robot. It is the term

we are going to estimate in this section. τ_f is the friction term.

To define the measurement part, the generalize momentum of the robot $\mathbf{p} = M(\mathbf{q})\dot{\mathbf{q}}$ is given. Besides, the differentiation with respect to time is shown as

$$\dot{\mathbf{p}} = \dot{M}(\mathbf{q})\dot{\mathbf{q}} + M(\mathbf{q})\ddot{\mathbf{q}} \quad (4)$$

Note that the passivity property, $(\dot{M} - 2C)$ is a skew-symmetric matrix. With the symmetry of M , we can conclude that

$$\dot{M} = C + C^T \quad (5)$$

Combing (3), (4) and (5), we can get

$$\dot{\mathbf{p}} = C(\mathbf{q}, \dot{\mathbf{q}})^T \dot{\mathbf{q}} - \mathbf{G}(\mathbf{q}) - \tau_f + \tau_m + \tau_h \quad (6)$$

Typically, the disturbance observer approach [12] and [13] involve joint acceleration and the inversion of the inertia matrix. Since the joint accelerations are calculated from the differentiation from the joint velocity, it usually amplifies the measurement noise of the signal. Besides, the latter requirement may be computationally costly especially when the manipulator is with high degrees of freedom. Inspired by the idea of [11], the generalized momentum is used to describe the manipulator dynamics to avoid the high computationally cost.

In this study, we assume the hypothesis model of interactive torque can be expressed as

$$\dot{\tau}_h = A_\tau \tau_h + \omega_h \quad (7)$$

where $A_\tau \in \mathbb{R}^{n \times n}$ and $\omega_h \sim N(0, Q_h)$ is the Gaussian white noise (or uncertainty). Considering that smooth movement is a characteristic feature of healthy and well-trained motor behavior [14], it implies that we can assume $A_\tau = 0_{n \times n}$. The estimated friction has the uncertainty which can be expressed as

$$\omega_p = \hat{\tau}_f - \tau_f \sim N(0, Q_p) \quad (8)$$

where ω_p is a Gaussian white noise and $\hat{\tau}_f$ is the estimated joint friction vector. Assuming that the estimated robot dynamics parameters are accurate enough so they can be seen as same as real robot dynamics parameter. Combing (6) and (8), the generalized momentum can be expressed as

$$\dot{\mathbf{p}} = \mathbf{u} + \tau_h + \omega_p \quad (9)$$

where \mathbf{u} is defined as

$$\mathbf{u} = \tau_m + C(\mathbf{q}, \dot{\mathbf{q}})^T \dot{\mathbf{q}} - \mathbf{G}(\mathbf{q}) - \hat{\tau}_f \quad (10)$$

Taking (7) and (9) into the state space form and adding the measurement equation, we obtain the following differential equations:

$$\begin{aligned} \begin{bmatrix} \dot{\mathbf{p}} \\ \dot{\tau}_h \end{bmatrix} &= \begin{bmatrix} 0_n & I_n \\ 0_n & A_\tau \end{bmatrix} \begin{bmatrix} \mathbf{p} \\ \tau_h \end{bmatrix} + \begin{bmatrix} I_n \\ 0_n \end{bmatrix} \mathbf{u} + \begin{bmatrix} \omega_p \\ \omega_h \end{bmatrix} \\ y &= [I_n \ 0_n] \begin{bmatrix} \mathbf{p} \\ \tau_h \end{bmatrix} + \mathbf{v} \end{aligned} \quad (11)$$

where $\mathbf{v} \sim N(0, R)$ is the measurement noise. Since \mathbf{q} and $\dot{\mathbf{q}}$ are available, $\mathbf{p} = M(\mathbf{q})\dot{\mathbf{q}}$ can be seen as a measurement in this system.

Finally, based on (11), the Kalman filter [15] can be constructed to estimate the states which include the interactive torque we aim to estimate.

C. Variable Admittance Model

After acquiring the estimated interactive torque between human and robot, we need to transfer the human intention into the desired joint angle and angular velocity. Admittance model mainly accepts a force as input and outputs a displacement. In [16], admittance model parameters (virtual inertia, virtual damping, and virtual stiffness) are fixed, which will result in the performance trade-off between fine movement and large movement. Regarding the disadvantage, we aim to eliminate this kind of performance trade-off as much as possible, so we implement a variable admittance model to achieve the better performance in both fine movement and large movement. The details about how to vary the parameters are discussed below.

Since the desired motion is free motion, we set the desired joint dynamics as a mass-damper system which can be expressed as

$$M_d(t)\ddot{\mathbf{q}}_d + D_d(t)\dot{\mathbf{q}}_d = \hat{\tau}_h \quad (12)$$

where $M_d(t)$ and $D_d(t)$ are the time-varying desired virtual mass matrix and time-varying desired virtual damping matrix, respectively. Moreover, both of them are set as a diagonal matrix that can be expressed as $M_d(t) = \text{diag}\{m_1, m_2 \dots, m_n\}$ and $D_d(t) = \text{diag}\{d_1, d_2 \dots, d_n\}$.

Equation (12) can be written in the Laplace domain as

$$\dot{Q}_{d,i}(s) = \frac{\frac{1}{d_i}}{\frac{m_i}{d_i}s + 1} \hat{\mathbf{T}}_{h,i}(s) \quad (13)$$

where $\dot{Q}_{d,i}(s)$ is the Laplace transform of $\dot{q}_{d,i}$ and $\hat{\mathbf{T}}_{h,i}(s)$ is the Laplace transform of $\hat{\tau}_{h,i}$. The subscript i indicates i -th joint. With (13), it can conclude that the desired virtual damper d_i affects the steady state value of $\dot{Q}_{d,i}(s)$ and the ratio of desired virtual mass to desired virtual damper $\frac{m_i}{d_i}$ affect the dynamics between $\dot{Q}_{d,i}(s)$ and $\hat{\mathbf{T}}_{h,i}(s)$.

Based on the above analyses, we construct the detailed formulation of the admittance parameters in two motion states, involving acceleration and deceleration, with definition σ_i as the moving state of the i -th joint. The motion state can be monitored by these equations

$$\sigma_i = \begin{cases} \text{acceleration,} & \text{if } \text{sgn}(\dot{q}_{d,i})\text{sgn}(\ddot{q}_{d,i}) = 1 \\ \text{deceleration,} & \text{if } \text{sgn}(\dot{q}_{d,i})\text{sgn}(\ddot{q}_{d,i}) = -1 \end{cases} \quad (14)$$

To improve the motion smoothness and responsiveness, the desired virtual damping should decrease while accelerating and increase while decelerating. Besides, it is recognized in the literature that the damping has a greater influence on the human perception [17], [18]. The desired virtual damping equation can be expressed as

$$\begin{aligned} d_i &= d_{f,i} - \alpha_{a,i} |\dot{q}_{d,i}|, \text{ for acceleration} \\ d_i &= d_{f,i} + \alpha_{d,i} |\dot{q}_{d,i}|, \text{ for deceleration} \end{aligned} \quad (15)$$

where $d_{f,i}$ is the default value of the desired virtual damping in the i -th joint, and $\alpha_{a,i}$, $\alpha_{d,i}$ are the weighting factor

for angular acceleration while accelerating or decelerating respectively. Both weighting factors are bounded from 0 to 1. For the acceleration phase, in order to maintain the same feeling for the user, the ratio of the desired virtual mass to virtual damping are held at the same constant. For the deceleration phase, increasing the damping and lowering the mass lead to the higher responsiveness. The desired virtual mass equation can be expressed as

$$\begin{aligned} m_i &= \frac{m_{f,i}}{d_{f,i}} d_i, \text{ for acceleration} \\ m_i &= \frac{m_{f,i}}{d_{f,i}} [1 - \beta(1 - \frac{d_{f,i}}{d_i})] d_i, \text{ for deceleration} \end{aligned} \quad (16)$$

where $m_{f,i}$ is the defaulted desired virtual mass and $\beta(0 < \beta < 1)$ is a parameter used to adjust the ratio of desired virtual mass to desired virtual damping. Although the setting of admittance model parameters [19] can be assisted by the human arm and the biomechanical data, the physical condition is varied from person to person. Instead of using the biomechanical data, we tune those default parameters by the subjects feeling and try to imitate the patients possible interactive torque which is smaller than the normal person.

D. Dithering Signal for Overcoming Static Friction

The dithering signal design here is to solve the limitation of the interactive torque observer arising when the joint is static. If the velocity in the i -th joint is zero, the y_i and $\hat{\tau}_{f,i}$ both become zero. Respecting to (11), this results that the estimate of the interactive torque depends incorrectly on the sum of the interactive torque and the static friction. As the result, the patient should first exert a large enough force to let the joint rotating and let the interactive torque observer start to work properly. The dithering signal is designed to be a square wave shape signal with high frequency, then feed-forward to the robot when the joint velocity is zero. It helps the patient overcome the static friction easily. Note that the magnitude needs to be smaller than the static friction in order not to make the joint move.

IV. EXPERIMENTAL RESULTS

In this section, two experiments are conducted to evaluate the performance of the interactive torque observer and the active mode therapy control scheme. We first explain the experiment setup and protocol, and then we give the experiment results and discussion.

A. Experiment Setup and Protocol

Since both of the experiment results are compared with [8], we will briefly discuss it. In [8], a generalized momentum interactive torque observer is constructed to conduct the active mode therapy. However, the method in [8] has two potential problems. First, the friction model does not consider the effect of the environment. Second, the control loop in [8] is simply enlarging the estimated interactive torque which may cause the unsmooth movement. Thus, instead of using the friction model in [8], we proposed a DNN based friction estimation to improve the model accuracy.

Moreover, we implement a variable admittance model to improve movement smoothness.

1) Protocol of experiment 1(Interactive torque observer):

Before we implement the interactive torque observer into the active mode therapy control, we have to make sure the quality of the interactive torque observer is good enough to replace the F/T sensor. Therefore, the first experiment is designed to evaluate the interactive torque observer performance on HABD, SF, and EF joint , and the results are compare with [8].

The experiment is that the robot tracks a reference trajectory with a constant angular velocity trajectory which will not be affected by the external force from the subject. To evaluate the performance of the observer, we divide the whole motion into two periods. Besides, the subject is instructed to apply different force in each motion period. The reason why the subject needs to apply the different direction force is that we intentionally let the subject imitate the patient behavior. The partial motion which starts from an origin point and moves to an end point is called as the first moving period. After the first moving period, the motion stops for 5 seconds and moves from an end point to origin point which is called as the second moving period. During the first moving period, we instruct the subject first to apply a period of force whose direction is the same as the moving direction of the robot and then apply a period of force whose direction is the opposite to the moving direction of the robot. In the second moving period, we direct the subject apply a period of force whose direction is the opposite of the movement first and then apply a period of force whose direction is the same as the moving direction of the robot. In the stop period, the subject applies no force. Remind that the trajectories are not influenced by the apply force because the velocity controller rejects the external force from the subject.

Since we focus on the accuracy of the estimation interactive torque, root-mean-square error (RMSE) and normalized root-mean-square error (NRMSE) are chosen to be the evaluation indices. RMSE is used to compare accuracy between proposed work and related work, and NRMSE is used to compare the performance between each joint. The reference interactive torque is computed from the F/T sensors. The experimental results will be shown in Section IV-B.

2) Protocol of experiment 2(Active mode control):

The second experiment is a point to point task which is designed to evaluate active mode control performance in Activities of Daily Living (ADL). The ADL is a term used in healthcare to refer to people's daily self-care activities. The ADL movements chosen in the experiment are reaching, feeding, and greeting. Here the analysis will focus on the feeding exercise. Feeding exercise composes of HABD and EF, note that SF and ER are fixed at 45 degrees and 70 degrees, respectively. The origin point and end point of HABD are 5 degrees and 75 degrees. The origin point and end point of EF are 0 degrees and 75 degrees. The exercise flow is shown in Fig. 6. During the experiments, we provide visual feedback which is the current joint angle for the patient.

We introduce two indices to evaluate the active mode



Fig. 6. The flow of feeding exercise.

exercises. The first index is called dimensionless jerk (DLJ) which is used to qualify the smoothness of the movement. The formulation of DLJ can be expressed as $DLJ \triangleq \frac{[n_2 - n_1 \cdot \Delta t]^3}{\omega_{peak}^2} \sum_{n_1}^{n_2} \ddot{\omega}(n)^2 \cdot \Delta t$, where $\omega(n)$ is the angular velocity in time step n . n_1, n_2 are the start and the end time steps of the movement and ω_{peak}^2 is the peak velocity during the movement. Note that the smaller the DLJ value, the smoother the motion is.

The second index is the average of the interactive torque between patient and robot which indicates the average torque subject exerted on the robot. The formulation can be expressed as $\tau_{avg} = \frac{\sum_T |\tau(t)|}{T}$, where T is the total time of the movement. A small value of τ_{avg} means the subject can complete the task easily.

There are 3 subjects, including one female and two male, conducting the experiment, and their ages are distributed from 22 to 24 years old. They do not have any upper-limb impairment and the experiments are conducted with their right-side arm.

B. Experiment Result & Discussion

1) Results of experiment 1(Interactive torque observer):

In Fig. 7, the experimental result of one constant velocity in HABD joint is presented. In this figure, the upper figure is the trajectory and the lower figure shows the interactive torque. The blue line, red line, and green line indicate estimated interactive torque of the [8], proposed observer, and F/T sensor, respectively. The evaluation results of interactive torque are shown in Table I and we can see that the interactive torque observer utilizing Kalman filter outperform [8]. Especially, the result of HABD joint is three times better than [8]. Besides, the SF and EF improve 70% and 40% of NRMSE, it verifies that utilizing Kalman filter can have better estimation accuracy. Moreover, we compare the interactive torque estimation with and without using proposed DNN friction model in Fig. 8. The quantitative results are shown in Table II. We can see that the interactive torque estimation is more accuracy with the proposed DNN friction model.

The main reasons for the better outcome of the proposed method in this paper are shown as follow. First, the accuracy of the friction model plays an important role in interactive torque observer, and the proposed DNN model of HABD joint perfectly estimates the friction. Second, regarding that we assume the dynamics of estimated interactive torque is zero, when the interactive torque is not changed, Kalman filter can trust more on the estimated value. Conclude both of the results and reasons above, the interactive torque observer utilizing Kalman filter have the ability to replace the F/T sensor to acquire human intention to some degree.

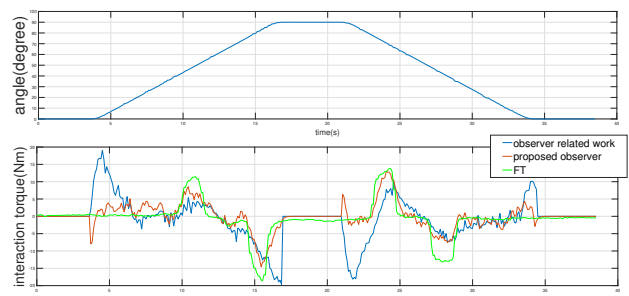


Fig. 7. Experiment result of interactive torque observer in HABD joint.

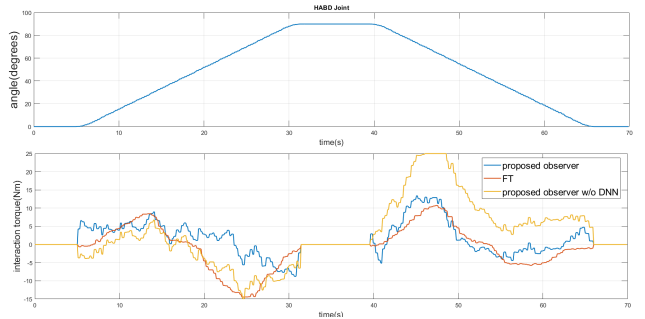


Fig. 8. Experiment result of interactive torque observer w/ and w/o DNN

2) *Results of experiment 2(Active mode control):* In Fig. 9, the trajectories are displayed in 2-dimensional joint space. The interactive torque of each joint is shown in Fig.10. The blue line is [8] and the red line is the proposed work in both figures. The average evaluation result is shown in Table III. From Fig. 9, we can see that the proposed method is better in moving multiple joints at the same time. From Fig. 10 and Table III, we can notice that the average of interactive torque results of our method in feeding exercise is smaller than [8] except for EF joint. The reason is that the EF of [8] is too easy for the subject to push, so it has lower results of interactive torque. However, it cause the problem that exoskeleton will first move the EF and then move another joint. Apparently, this situation reflects on the poor smoothness, so the DLJ index of the proposed method is better than [8]. Overall, the proposed method still has the smoother, faster movement and lower average torque needed to complete the task.

TABLE I
EXPERIMENT RESULT OF INTERACTIVE TORQUE OBSERVER.

Joint	Index	Related Work	Proposed Work
HABD	RMSE (Nm)	8.44	2.69
	NRMSE	0.29	0.09
SF	RMSE (Nm)	4.16	2.29
	NRMSE	0.12	0.07
EF	RMSE (Nm)	2.70	1.83
	NRMSE	0.14	0.10

TABLE II
EXPERIMENT RESULT OF OBSERVER W/ AND W/O DNN.

Joint	Index	without DNN	with DNN
HABD	RMSE (Nm)	6.94	4.45
	NRMSE	0.28	0.18

TABLE III

AVERAGE EVALUATION RESULT IN FEEDING EXERCISE OF ALL SUBJECTS

ADL	Joint	Index	Related Work	Proposed
Feeding	HABD	DLJ	5713.40	4590.37
		Avg. Torque (Nm)	5.89	5.47
	EF	DLJ	12243.50	4877.80
		Avg. Torque (Nm)	2.91	3.22

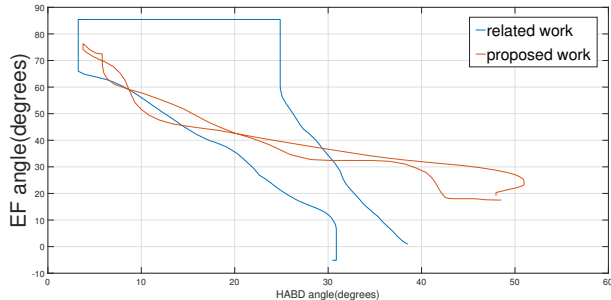


Fig. 9. The experiment result of feeding in active mode.

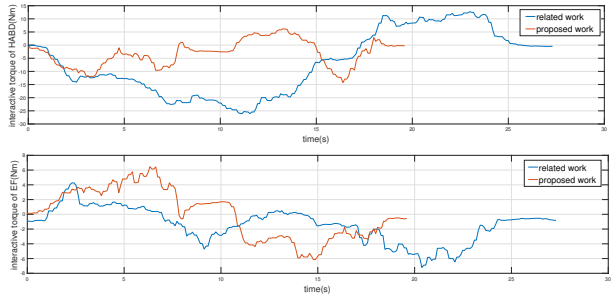


Fig. 10. The experiment result of feeding in active mode.

V. CONCLUSION

In this paper, a sensorless exoskeleton robot control with friction estimation for active mode upper-limb rehabilitation is proposed. In order to conduct an active mode therapy, an interactive torque observer utilizing Kalman filter with the DNN based friction model estimation is constructed to extract human intention. According to the experiment results, the performance of the interactive torque observer in this paper achieves satisfactory performance in both single and multi-joint movements. Moreover, the variable admittance model implemented in the control scheme preserves the fine and smooth movement. In conclusion, the proposed method has the capability to spare the F/T sensor on the exoskeleton, which not only solves the contacting point problem but also lowers the cost of exoskeleton construction. In future work, in order to evaluate the performance of proposed system on both normal and injured subjects the conduction on clinical rehabilitation will be considered.

VI. ACKNOWLEDGEMENT

This research was supported by the Joint Research Center for AI Technology and All Vista Healthcare under Ministry of Science and Technology of Taiwan, and Center for Artificial Intelligence & Advanced Robotics, National Taiwan University, under the grant numbers of 108-2634-F-002-016 and 108-2634-F-002-017.

REFERENCES

- [1] R. Lugo, P. Kung, and C. B. Ma, "Shoulder biomechanics," *European journal of radiology*, vol. 68, no. 1, pp. 16-24, 2008.
- [2] M. Cirstea and M. F. Levin, "Compensatory strategies for reaching in stroke," *Brain*, vol. 123, no. 5, pp. 940-953, 2000.
- [3] V. S. Huang and J. W. Krakauer, "Robotic neurorehabilitation: a computational motor learning perspective," *The journal of neuroengineering and rehabilitation*, vol. 6, no. 1, p. 5-17, 2009.
- [4] J. McCabe, M. Monkiewicz, J. Holcomb, S. Pundik, and J. J. Daly, "Comparison of robotics, functional electrical stimulation, and motor learning methods for treatment of persistent upper extremity dysfunction after stroke: a randomized controlled trial," *Archives of physical medicine and rehabilitation*, vol. 96, no. 6, pp. 981-990, 2015.
- [5] S. Wang, J. Li, Y. Zhang, and J. Wang, "Active and Passive Control of an Exoskeleton with Cable Transmission for Hand Rehabilitation," *International Conference on Biomedical Engineering and Informatics*, pp. 1-5, 2009.
- [6] W. Yu and J. Rosen, "Neural PID control of robot manipulators with application to an upper limb exoskeleton," *IEEE Transactions on cybernetics*, vol. 43, no. 2, pp. 673-684, 2013.
- [7] S. Tominaga, H. Nakamura, N. Mizutani, R. Sakamoto, K. i. Yano, T. Aoki, and Y. Nishimoto, "Elbow joint motion support for C4 level cervical cord injury patient using an exoskeleton robot," *IEEE International Conference on Robotics and Automation (ICRA)*, pp. 4979-4984, 2015.
- [8] Lee-Kai Liu, Li-Yu Chien, Shang-Heh Pan, Jia-Liang Ren, Chi-Lun Chiao, Wei-Hsuan Chen, Li-Chen Fu and Jin-Shin Lai, "Interactive torque controller with electromyography intention prediction implemented on exoskeleton robot NTUH-II," *IEEE International Conference on Robotics and Biomimetics (ROBIO)*, 2017.
- [9] Chia-Hsun Lin, Wei-Ming Lien et al., "NTUH-II robot arm with dynamic torque gain adjustment method for frozen shoulder rehabilitation," *IEEE International Conference on Intelligent Robots and Systems*, 2014.
- [10] A. Wahrburg, E. Morara, G. Cesari, B. Matthias, and H. Ding, "Cartesian contact force estimation for robotic manipulators using kalman filters and the generalized momentum," *IEEE International Conference on Automation Science and Engineering (CASE)*, pp. 1230-1235, 2015.
- [11] A. De Luca and R. Mattone, "Actuator failure detection and isolation using generalized momenta," *Proceedings of IEEE International Conference on Robotics and Automation*, vol. 1, pp. 634-639, 2003.
- [12] K. S. Eom, I. H. Suh, W. K. Chung, and S.-R. Oh, "Disturbance observer based force control of robot manipulator without force sensor," *Proceedings of IEEE International Conference on Robotics and Automation*, vol. 4, pp. 3012-3017, 1998.
- [13] A. Colom, D. Pardo, G. Alenya, and C. Torras, "External force estimation during compliant robot manipulation," *International Conference on Robotics and Automation (ICRA)*, pp. 3535-3540, 2013.
- [14] T. J. Sejnowski, "Neurobiology: making smooth moves," *Nature*, vol. 394, no. 6695, p. 725, 1998.
- [15] G. Bishop and G. Welch, "An introduction to the Kalman filter," *Proceedings of SIGGRAPH Course*, vol. 8, no. 27599-23175, p. 41, 2001.
- [16] C. Carignan, J. Tang, and S. Roderick, "Development of an exoskeleton haptic interface for virtual task training," *IEEE/RSJ International Conference on Intelligent Robots and Systems(IROS)*, pp. 3697-3702, 2009.
- [17] R. Ikeura, H. Monden, and H. Inooka, "Cooperative motion control of a robot and a human," *Proceedings of 3rd IEEE International Workshop on Robot and Human Communication*, pp. 112-117, 1994.
- [18] V. Duchaine and C. M. Gosselin, "General model of human-robot cooperation using a novel velocity based variable impedance control," *Proceedings of EuroHaptics Conference and Symposium on Haptic Interfaces for Virtual Environment and Teleoperator Systems*, p.446 - 451, 2007.
- [19] W. Yu, J. Rosen, and X. Li, "PID admittance control for an upper-limb exoskeleton," *American Control Conference (ACC)*, pp. 1124-1129, 2011